HHS Public Access

Author manuscript

Mol Cell. Author manuscript; available in PMC 2017 May 05.

Published in final edited form as:

Mol Cell. 2016 May 5; 62(3): 397–408. doi:10.1016/j.molcel.2016.04.001.

Structural basis for non-canonical substrate recognition of cofilin/ADF proteins by LIM kinases

Stephanie Hamill[1], **Hua Jane Lou**[1], **Benjamin E. Turk**[1,3], and **Titus J. Boggon**[*,1,2,3]

[1]Department of Pharmacology, Yale University School of Medicine, New Haven, CT 06520

[2]Department of Molecular Biophysics and Biochemistry, Yale University School of Medicine, New Haven, CT 06520

[3]Yale Cancer Center, Yale University School of Medicine, New Haven, CT 06520

SUMMARY

Cofilin/actin-depolymerizing factor (ADF) proteins are critical nodes that relay signals from protein kinase cascades to the actin cytoskeleton, in particular through site-specific phosphorylation at residue Ser3. This is important for regulation of the roles of cofilin in severing and stabilizing actin filaments. Consequently, cofilin/ADF Ser3 phosphorylation is tightly controlled as an almost exclusive substrate for LIM kinases. Here we determine the LIMK1:cofilin-1 co-crystal structure. We find an interface that is distinct from canonical kinase-substrate interactions. We validate this previously unobserved mechanism for high fidelity kinase-substrate recognition by *in vitro* kinase assays, examination of cofilin phosphorylation in mammalian cells, and functional analysis in *S. cerevisiae*. The interface is conserved across all LIM kinases. Remarkably, we also observe both pre- and post-phosphotransfer states in the same crystal lattice. This study therefore provides a molecular understanding of how kinase-substrate recognition acts as a gatekeeper to regulate actin cytoskeletal dynamics.

INTRODUCTION

Fidelity in protein kinase signaling is achieved both at a systems level and at the molecular level. At the systems level, mechanisms such as protein expression, targeting, scaffolding, and competition all play roles in achieving fidelity, while at the molecular level direct

*To who correspondence should be addressed: titus.boggon@yale.edu.

ACCESSION NUMBERS

Accession codes: The structure of pLIMK1$_{CAT}^{D460N}$:Cofilin is deposited in the Protein Data Bank under accession code 5HVK, and LIMK1$_{CAT}^{D460N}$ is deposited under accession code 5HVJ.

SUPPLEMENTAL INFORMATION

Supplemental information includes Supplemental Experimental procedures and 5 figures.

AUTHOR CONTRIBUTIONS

S.H. and T.J.B. conceived the project. S.H., B.E.T. and T.J.B. conceived and designed the experiments. S.H. and H.J.L. performed the experiments. S.H., H.J.L., B.E.T. and T.J.B. analyzed the experiments. S.H. sub-cloned, expressed, purified, crystallized, solved the structures, and conducted the kinase assays. H.J.L. performed the yeast growth assays. S.H., B.E.T. and T.J.B. wrote the paper.

interactions between the kinase and substrate define the pairwise kinetics of catalysis (Ubersax and Ferrell, 2007). The molecular level specificity determinants can be divided into distal ‘docking’ interactions and phosphosite ‘linear motif’ interactions with the kinase catalytic cleft (Ubersax and Ferrell, 2007), both of which have been well studied structurally. Docking interactions typically occur between substrate residues distal from the phosphorylation site and kinase domain regions outside of the catalytic cleft, but can also involve adaptor or scaffolding proteins (Bhattacharyya et al., 2006; Remenyi et al., 2006). Linear motif interactions occur between an extended peptide encompassing up to 5 residues N- and C-terminal of the phosphoacceptor site and a region immediately adjacent to the kinase catalytic center (Bose et al., 2006; Goldsmith et al., 2007). The LIM kinases, which play crucial roles in regulation of actin dynamics show exquisite fidelity in phosphorylation of cofilin/ADF (actin-depolymerizing factor) proteins in a manner that does not appear to fit either of these paradigms for kinase substrate recognition (Amano et al., 2001; Mezna et al., 2012). Cofilin/ADF proteins are processed to remove the N-terminal initiator methionine residue, leaving only a single amino acid residue N-terminal to the LIM kinase phosphorylation site, Ser3 (Agnew et al., 1995; Kanamori et al., 1998). As a result, this kinase/substrate interaction cannot be guided by typical linear motif interactions, and there are no evident opportunities for docking interactions through other domains. The high specificity of LIM kinases for Ser3 in their cofilin/ADF substrates is therefore likely to involve features absent from other kinase-substrate pairs.

Phosphorylation of cofilin/ADF proteins at Ser3 is crucial for regulating their direct interaction with actin (Agnew et al., 1995; Morgan et al., 1993; Ressad et al., 1998). The cofilin/ADF proteins are critical mediators of actin depolymerization (Bravo-Cordero et al., 2013; Edwards et al., 1999; Maekawa et al., 1999), and their interaction with actin filaments induces conformational changes in the filament that promote disassembly (Andrianantoandro and Pollard, 2006; Bamburg et al., 1999; De La Cruz, 2009; Elam et al., 2013). Ser3 phosphorylation blocks this interaction without a change in cofilin structure (Blanchoin et al., 2000b), thereby serving as the key convergence point for the many signaling pathways that control actin cytoskeletal dynamics through cofilin/ADF proteins (Bravo-Cordero et al., 2013; Poukkula et al., 2011). The phosphorylation and dephosphorylation of cofilin/ADF is mediated by the LIM kinases and slingshot phosphatases, respectively (Arber et al., 1998; Niwa et al., 2002; Yang et al., 1998). The four LIM kinase family members (LIMK1, LIMK2 and testicular protein kinases TESK1 and TESK2)(Mizuno et al., 1994; Okano et al., 1995; Rosok et al., 1999; Toshima et al., 1995) demonstrate exquisite substrate specificity for Ser3 of cofilin/ADF (Mizuno, 2013; Scott and Olson, 2007)(Figure 1), with only two other cellular substrates reported (p25/TPPP and CREB)(Acevedo et al., 2007; Yang et al., 2004).

In this study we define the molecular basis for this almost exclusive kinase-substrate relationship by determining the co-crystal structure of the LIMK1 catalytic domain in complex with cofilin-1. The structure reveals that specificity is driven by an interaction between a region of the LIM kinase catalytic domain C-lobe that adopts an atypical conformation, and the actin binding helix of cofilin. Targeted mutations at this interface disrupt cofilin-1 phosphorylation by LIMK1 *in vitro* and in mammalian cells, and block functional inactivation of cofilin-1 by LIMK1 in yeast. Our crystal structure reveals a

mechanism by which protein-kinase fidelity can be encoded, where specificity is defined by a helix spatially, but not sequentially, proximal to the phosphate acceptor residue. This arrangement represents a previously unappreciated mechanism of achieving kinase-substrate fidelity and is fundamental to proper regulation of cofilin/ADF proteins by LIM kinases.

RESULTS

Preparation of LIMK1 catalytic domain and cofilin-1 for co-crystallization

In our initial efforts to study the specificity of LIM kinases for cofilin/ADF proteins, we co-crystallized the LIMK1 kinase domain harboring a D460N kinase-inactivating point mutation ($LIMK1_{CAT}^{D460N}$) with a 9 amino acid peptide (ASGVTVNDE) corresponding to residues 2 – 10 of human cofilin-2. After determining the structure to 2.2 Å resolution (Table 1), we could not discern any electron density for the cofilin-2 peptide bound to the inactive LIMK kinase domain. We reasoned that activation loop phosphorylation of LIMK1 (at Thr-508) might promote interaction with cofilin by stabilizing the active conformation, and found that $LIMK1_{CAT}^{D460N}$ could be phosphorylated efficiently by the purified active PAK4 kinase domain (Ha et al., 2012), as shown in Figure S1. Mass spectrometry confirmed a single phosphate addition to activation loop Thr-508, allowing purification of homogeneous crystallization-quality $pLIMK1_{CAT}^{D460N}$ (not shown). We also generated full-length human cofilin-1 (without N-terminal modification) using the SUMO expression and proteolysis system. Although not N-acetylated, this full-length cofilin was efficiently phosphorylated by the wild-type LIMK1 kinase domain (termed $LIMK1_{CAT}$) (see Figure 3D for example), suggesting it to be suitable for co-crystallography with the LIMK1 kinase domain.

Co-crystal structure of LIMK1 catalytic domain with full-length cofilin-1

Co-crystals of $pLIMK1_{CAT}^{D460N}$ with cofilin-1 grew in the presence of $MgCl_2$ and the generally non-hydrolyzable ATP analogue, adenosine-5′-(β,γ-imido)triphosphate (AMP-PNP), where the atom linking the β- and γ- phosphates is a nitrogen (Yount et al., 1971). Diffraction data from four crystals were merged together (Table 1) and a molecular replacement solution obtained. The resulting structure contains two LIMK1:cofilin heterodimers per asymmetric unit (Figure 2A). LIMK1 in each heterodimer folds as a canonical protein kinase domain, consisting of a β-strand rich N-lobe and an α-helix rich C-lobe. The LIMK1 molecules unambiguously show nucleotide bound in the ATP-cleft, phosphorylation of Thr508 in the activation loop, and a ‘DFG-in’ conformation. For protein kinases, the location of helix αG is usually proximal to the C-terminus of the activation segment, however, in LIMK1 helix αG is observed distal from the activation loop, which we discuss below. Our structures of apo and cofilin-bound LIMK1 are conformationally similar, with root mean square (rms) deviations of 0.8 – 1.1 Å over 266 – 273 Cα atoms.

In each heterodimer, cofilin adopts the canonical ADF/cofilin fold, with a central 6-stranded β-sheet surrounded by five α-helices. The two copies of cofilin show rms deviation of 0.6 Å over 159 Cα atoms, and comparison with previously determined structures of cofilin/ADF proteins show highest similarity to uncomplexed structures of human cofilin-1 (Klejnot et al., 2013) (PDB ID: 4BEX, rms deviation 1.1 – 1.3 Å over 163 Cα), *Acantamoeba polyphaga* actophorin (Blanchoin and Pollard, 1998) (PDB ID: 1CNU, rms deviation 1.4 –

1.5 Å over 131 Cα) and yeast cofilin (Fedorov et al., 1997) (PDB ID: 1CFY, rms deviation 1.5 Å over 130 Cα) suggesting that cofilin/ADF proteins undergo no major structural rearrangement on binding to LIM kinase.

The LIMK1:cofilin-1 co-crystal structure captures both pre- and post-catalytic states

The LIMK1:cofilin-1 co-crystal structure unexpectedly revealed clear transfer of the γ-phosphate of AMP-PNP to Ser3 of cofilin-1 in one of the two heterodimers; consequently the two complexes in the asymmetric unit are $pLIMK1_{CAT}^{D460N}$:cofilin-1:AMP-PNP (pre-catalysis) and $pLIMK1_{CAT}^{D460N}$:pSer3-cofilin-1:AMP-PN (post-catalysis) (Figure 2B,C, Figure S2A,B). We validated the presence of cofilin-1 pSer3 in the co-crystals by Western blot, and also that transfer had occurred in the crystallization drop and not during protein preparation (Figure S2C). This phosphotransfer event occurred despite our use of catalytically inactive $pLIMK1_{CAT}^{D460N}$ in the presence of AMP-PNP. Although the observation of phosphotransfer is unexpected, we note that while canonical kinase-inactivating mutations significantly reduce catalytic activity (including D→N mutation in the HRD-motif that we used), previous studies have reported residual, low levels of catalytic activity (Adams, 2001; Gibbs and Zoller, 1991; Skamnaki et al., 1999; Williams and Cole, 2002), and some kinases (for example, the low activity receptor tyrosine kinase ErbB3 (Kraus et al., 1989; Shi et al., 2010)) have Asn at this location. Likewise, the ATP-analogue AMP-PNP has reduced, but not abrogated, efficiency as a substrate compared to ATP, and *in crystal* kinase activity has previously been observed between the catalytic subunit of cAMP-dependent protein kinase (PKA) and a peptide substrate in the presence of AMP-PNP (Bastidas et al., 2013). The LIMK1:cofilin-1 co-crystal structure is a highly unusual instance where pre- and post-phosphorylation states of a kinase-substrate pair are both observed in the same crystal lattice.

Despite the moderate resolution of the structure (3.5 Å) we observe conformational differences between the pre- and post-catalysis complexes which are supported by the $2mF_{obs}$-DF_{calc}, mF_{obs}-DF_{calc}, and simulated annealing omit maps. Broadly, the pre-catalytic state of LIMK1 appears more competent for phosphotransfer than the post-catalytic state. In the pre-catalytic state the DFG-motif Asp (Asp478) and VAIK-motif Lys (Lys368) are oriented to coordinate substrate and Mg^{2+}, but are found to have shifted conformation in the post-catalysis state. Similarly, the glycine-rich P-loop is shifted in the post-catalytic state, and the adenine ring of the nucleotide moiety skews by approximately 10° between the pre- and post-catalytic states. Although these differences could potentially be due to crystal packing, we note that limited crystal packing interactions are observed in the region of the P-loop, β3-αC loop and αC-helix (Figure S2D). The differences between the pre- and post-catalysis structures are consistent with post-catalysis opening of the kinase domain towards release of the diphosphate nucleotide.

Structural basis for LIM kinase specificity for cofilin/ADF proteins

The co-crystal structure of $pLIMK1_{CAT}^{D460N}$ with cofilin-1 provides a clear description of how the LIM kinases recognize cofilin/ADF proteins with high fidelity, and how the kinase is directed to specifically phosphorylate Ser3. A highly complementary hydrophobic interaction between LIMK1 and cofilin precisely orients cofilin Ser3 to the correct location

for phosphotransfer to occur (Figure 3A, main panel). Importantly, the location of cofilin's interaction surface is structurally proximal, but sequentially distal, to Ser3. This interaction is observed in both complexes in the asymmetric unit, irrespective of pre- or post-catalysis state.

Cofilin/ADF proteins fold with their actin-binding helix α5 structurally proximal to the phosphoacceptor residue, Ser3. Indeed, in all of the solved structures of cofilin/ADF family proteins, the residue equivalent to Val-5 (human cofilin-1 numbering) is sandwiched between helix α5 and the β2-β3 loop (Klejnot et al., 2013)(Figures 3A, zoom 1, and Figure S3A). This essentially invariant cofilin fold restricts the conformational freedom of the phosphoacceptor residue Ser3, placing it perpendicular to helix α5, extending away from the cofilin domain (Figure S3A). This is a unique conformation for a kinase-substrate pair; usually complementary interactions are formed between the linear motif and the kinase domain, including a short β-sheet with the C-terminus of the activation loop (Ubersax and Ferrell, 2007)(Figure S3B). In view of this conserved sequence and fold of cofilin/ADF proteins, where only one amino acid is present N-terminal to the Ser3 phosphosite and residues C-terminal of Ser3 are buried in the hydrophobic core of the cofilin fold, it is not surprising that a non-canonical kinase-substrate interaction occurs.

Cofilin helix α5 acts as a guide to orient Ser3 to the correct location for phosphotransfer. This helix docks into a hydrophobic groove on the C-lobe of LIMK1 (Figure 3B) that is created by the C-terminal portion of the activation segment and an unusual conformation of the αFG loop (Figure 3A, zoom 1), and buries approximately 660 $Å^2$ on LIMK1 and 710 $Å^2$ on cofilin helix α5 for a total buried surface area of ~1370 $Å^2$. Cofilin helix α5 extends residues Leu111, Met115 and Ser119 into the groove (Figure 3A, zoom 2) from three successive turns of the helix, with Met115 deeply buried between LIMK1 residues Pro513, Tyr514, Ile521, Pro550, and Phe559 (Figure 3A). Further contacts are also made between the C-terminus of cofilin helix α5 and the β3-αC loop of the kinase N-lobe (Figure 3A, zoom 1), and polar interactions are observed between cofilin Lys112 and LIMK1 Asp549 and Asp551 (Figure 3A, zoom 3). Most of these residues are highly conserved in cofilin (Figure S3C). Comparison of LIMK1 with previous structures of LIM kinase domains, which are either phosphorylated or unphosphorylated on their activation loops (PDB IDs: 3S9S, 4TPT and the apo structure described here), show that no induced fit conformational changes occur in the C-lobe on binding to cofilin (Figure S3D). Indeed the unusual conformation of the αFG loop that forms the cofilin-binding hydrophobic groove seems to be stabilized by two conserved proline residues (Pro550 and Pro554), and by extensive polar interactions of Arg555 with backbone carbonyls which provides a base to the groove (Figure 3A, zoom 3). The co-crystal structure therefore suggests that both cofilin/ADF proteins and the catalytic domains of LIM kinases are conformationally poised and accessible for direct interaction with one another.

Mutations in LIM kinase C-lobe and cofilin helix α5 disrupt *in vitro* kinase activity

Purified LIMK1 kinase domain is generally a poor enzyme in kinase assays when short peptides or non-cofilin/ADF proteins are used as substrate, and we were unable to detect activity with either a cofilin Ser3-derived peptide or random peptide libraries (not shown). In

contrast, using purified pLIMK1$_{CAT}$ and full-length cofilin-1 we observe robust kinase activity, and Western blot analysis confirmed that LIMK1 phosphorylated cofilin-1 on Ser3 (Figure 3D,E). We hypothesized that efficient phosphorylation of the authentic substrate cofilin was attributable to our crystallographically-defined interaction surface. We therefore probed the importance of this interface by testing the ability of LIMK1 to phosphorylate cofilin-1 following incorporation of structurally-guided point mutations into either protein.

We designed two sets of complementary point mutations that we hypothesized would impair the interaction if used individually, but when used as a complementary pair might restore kinase activity. The first set aimed to disrupt and reconstitute an interaction between LIMK1 Met516 and cofilin-1 Ser119 by reversing the methionine and serine residues with LIMK1 M516S (LIMK1$_{CAT}^{M516S}$) and cofilin-1 S119M (cofilin^{S119M}) substitutions. The second set was designed to interrupt and restore polar interactions between LIMK1 residues Asp549/Asp551 and cofilin-1 residue Lys112, by incorporation of LIMK1 DD549/551KK (LIMK1$_{CAT}^{DDKK}$) and cofilin-1 K112D (cofilin^{K112D}) mutations. We confirmed intrinsic autophosphorylation activity of both LIMK1$_{CAT}^{M516S}$ and LIMK1$_{CAT}^{DDKK}$ (Figure S3E,F) and then tested the ability of the mutants to impact LIMK1 phosphorylation of cofilin. Individually, purified proteins with either set of LIMK1 mutation (LIMK1$_{CAT}^{M516S}$ and LIMK1$_{CAT}^{DDKK}$) displayed significant reduction in phosphorylation of wild-type cofilin. Likewise, purified cofilin-1 mutants (cofilin^{S119M} or cofilin^{K112D}) were significantly negatively impacted in their ability to be phosphorylated by wild-type LIMK1 (Figure 3C,D). In contrast, when we conducted kinase assays with either set of complementary mutation (LIMK1$_{CAT}^{M516S}$/cofilin^{S119M} and LIMK1$_{CAT}^{DDKK}$/cofilin^{K112D}) we observed full or partial restoration of kinase activity suggesting that the complementary mutation pairs can restore the ability of LIMK1 to phosphorylate cofilin-1 *in vitro*.

We next tested the importance of cofilin residue Met115 on kinase-substrate recognition. Met115 is buried deep into the hydrophobic groove of LIMK1 (Figure 3A) so we hypothesized that it might be key to the interface, and consequently LIMK1 recognition and phosphorylation of cofilin. We tested the ability of LIMK1 to phosphorylate a M115A mutant of cofilin (cofilin^{M115A}) and found that introduction of this mutation shows essentially complete loss of cofilin phosphorylation by LIMK1, indicating the critical importance of this residue for LIMK1 recognition of cofilin-1 (Figure 3D,E).

Targeted disruption of cofilin phosphorylation in cultured mammalian and yeast cells

To examine whether our crystallographically-defined interaction mode was relevant to cofilin phosphorylation by LIM kinases in cells as well as *in vitro*, we initially tested the ability of cofilin mutations to disrupt its phosphorylation by endogeneous LIM kinases in mammalian cells. Exogenously expressed hexahistidine-tagged cofilin was robustly phosphorylated at Ser3 in HEK293T cells by endogenous LIM kinases (Figure 4A), supporting previous studies (Edwards et al., 1999; Li et al., 2006). Confirming the crystallographically-defined interface in mammalian cells, we again found that mutation of cofilin Met115 severely affects the ability of cofilin to be phosphorylated on Ser3 (Figure 4A,B). Likewise, cofilin^{K112D} and cofilin^{S119M} also showed reduced Ser3 phosphorylation.

To further confirm the functional importance of the structurally-defined interaction mode for cofilin phosphorylation by LIM kinases, we reconstituted the mammalian LIMK1-cofilin pathway in the budding yeast *Saccharomyces cerevisiae*. The sole *S. cerevisiae* cofilin, Cof1, is essential for viability, and expression of mammalian cofilin-1 can rescue the growth defect of *cof1* mutant yeast (Iida et al., 1993; Moon et al., 1993). Furthermore, while mutation of Ser3 to Ala did not affect the ability of mammalian cofilin-1 to function in yeast, mutation to a phosphomimetic Asp residue abrogated its ability to support growth of a *cof1* mutant strain (Moriyama et al., 1996). Yeast lack obvious LIM kinase homologs, we therefore hypothesized that expression of human LIMK1 catalytic domain would phosphorylate and inactivate co-expressed human cofilin, thus preventing cofilin from rescuing growth in an inviable *cof1* mutant strain. We used a strain harboring a temperature sensitive *COF1* allele (*cof1-ts*), which grows normally at 25°C but fails to grow at 37°C due to inactivation of the mutant Cof1 protein (Lappalainen et al., 1997). This strain was transformed with plasmids for constitutive expression of human cofilin-1 and galactose-inducible expression of human $LIMK1_{CAT}$, and assessed for growth at the restrictive temperature following galactose induction. As expected, we found that expression of human cofilin supports growth of the *cof1-ts* strain at 37 °C (Figure 4C). However, co-expression of $LIMK1_{CAT}$ in this context abolishes growth. Importantly, mutation of Ser3 of human cofilin to Ala in this system rescued growth upon co-expression $LIMK1_{CAT}$, indicating that $LIMK1_{CAT}$ inhibits growth by direct phosphorylation of cofilin and not through non-specific toxicity. This assay therefore allowed us to probe the crystallographically observed LIMK1-cofilin interaction *in vivo*.

We initially examined the behavior of human cofilin-1 mutants that impacted phosphorylation by LIMK1 *in vitro* (K112D, M115A, and S119M, Figure 3). All human cofilin-1 mutants tested were capable of supporting the growth of *cof1-ts* yeast at 37 °C, suggesting that disruption of the LIMK1 binding interface does not affect the ability of cofilin to regulate actin filament dynamics. Expression of $cofilin^{K112D}$ or $cofilin^{M115A}$ partly rescued the ability of yeast to grow when co-expressed with wild-type $LIMK1_{CAT}$, suggesting a significant impairment in the ability of LIMK1 to inactivate cofilin (Figure 4D). The partial rescue afforded by these mutants suggests residual phosphorylation of cofilin-1 despite a reduced rate of phosphorylation, which is likely to be a consequence of high level expression of $LIMK1_{CAT}$. In contrast to the other mutants tested, $cofilin^{S119M}$ was fully inactivated by $LIMK1_{CAT}$ expression in yeast. These results are consistent with the central role for Met115 in the cofilin-LIMK1 interface. We also examined the effect of LIMK1 mutations that disrupt phosphorylation of cofilin *in vitro* (Figure 4E). Expression of $LIMK1_{CAT}^{DDKK}$ had no affect on the ability of human cofilin to rescue *cof1-ts* growth, suggesting complete loss of Ser3 phosphorylation. $LIMK1_{CAT}^{M516S}$ was partly impaired in suppressing growth, suggesting a partial decrease in phosphorylation. Co-expression of $cofilin^{K112D}$ with $LIMK1_{CAT}^{DDKK}$ did not restore growth suppression (not shown), consistent with the low level of Ser3 phosphorylation observed *in vitro* (Figure 3). Overall, these results indicate that disruption of the crystallographically-observed LIMK1-cofilin interaction, particularly by the cofilin M115A mutation, deleteriously impacts the ability of LIMK1 to inactivate cofilin-1 *in vivo*.

The LIMK1:cofilin-1 co-crystal structure defines the structural basis for LIM kinase family phosphorylation of cofilin/ADF proteins

The LIM kinase sub-group of protein kinases contains LIMK1, LIMK2 and the related TESK1 and TESK2. We conducted sequence alignment followed by conservation mapping onto the surface of LIMK1 in the co-crystal structure and found essentially complete conservation of the cofilin/ADF-binding surface between LIMK1/2 and TESK1/2. This indicates an evolutionary requirement for this arrangement of surface amino acids, presumably in order to bind cofilin/ADF proteins (Figure 5A, Figure S4). To confirm that the mechanism of cofilin/ADF protein recognition is conserved across the group we conducted *in vitro* kinase activity assays. We expressed and purified the catalytic domain of TESK1 ($TESK1_{CAT}$) and used wild-type or mutant purified cofilin-1 as substrates ($cofilin^{M115A}$, $cofilin^{K112D}$, $cofilin^{S119M}$). We found that $TESK1_{CAT}$ could efficiently phosphorylate wild-type cofilin-1, but that each of the cofilin mutants showed significantly less phosphorylation (Figure 5B,C). We therefore propose that the LIMK1:cofilin-1 co-crystal structure defines the class for LIM kinase family phosphorylation of cofilin/ADF proteins.

DISCUSSION

Insights into control of actin regulation by high fidelity phosphorylation of cofilin

Signal transduction to the actin cytoskeleton is critical for regulation of a wide array of cellular outcomes, and many kinase cascades control filament turnover by regulating the phosphorylation of cofilin/ADF proteins (Figure 1). The nodal point for these pathways is a high fidelity kinase-substrate pairing between the LIM kinase sub-group of serine-threonine kinases and residue Ser3 of the cofilin/ADF proteins, however, the molecular basis for how this pairing is achieved has remained perplexing. In the current study we determined the co-crystal structure of LIMK1 catalytic domain in complex with full-length cofilin-1 and found that the specificity is defined by a highly complementary interaction between the kinase C-lobe and the cofilin actin-binding helix. This interaction acts as a guide to place the phosphoacceptor cofilin Ser3 residue in precisely the correct location for phosphotransfer to occur.

Phosphorylation of cofilin/ADF proteins is a key mechanism for regulating the actin cytoskeleton. Cofilin/ADF proteins can bind directly both to globular and to filamentous actin. They induce conformational changes in filaments that promote ‘actin aging’ by promoting dissociation of Pi from ADP-Pi actin filaments (Blanchoin and Pollard, 1999). Cofilin binds more strongly to ADP-actin filaments and induces a twist in the filament to initiate severing (Andrianantoandro and Pollard, 2006; Bamburg et al., 1999; Blanchoin et al., 2000a; De La Cruz, 2009; Elam et al., 2013; Poukkula et al., 2011). Alongside phosphorylation of residue Ser3, control of cofilin/ADF binding to filamentous actin is also regulated by interaction of phosphoinositides (Ojala et al., 2002; Van Troys et al., 2008; Yonezawa et al., 1990; Zhao et al., 2010), interaction with cortactin (Oser et al., 2009) and changes in intracellular pH (Bernstein et al., 2000), however, cofilin Ser3 phosphorylation is the focal regulation point for transduction of extracellular signals to changes in the actin cytoskeleton, and plays a critical role in regulation of actin (Bravo-Cordero et al., 2013). Our

study shows how this array of signals achieves a discrete and targeted impact on a single phosphoacceptor site.

Actin competes with LIM kinase phosphorylation of cofilin/ADF proteins

The structure of LIMK1 with cofilin-1 shows that the actin-binding helix (α5) of cofilin is required to mediate the interaction. Previous studies have shown that helix α5 is required for the interaction of cofilin/ADF proteins with either globular or filamentous actin (Bravo-Cordero et al., 2013), and the co-crystal structure of twinfilin with actin suggests that the residue analogous to Met115 in cofilin is important for the interaction, suggesting an overlapping actin-binding surface (Paavilainen et al., 2008). Therefore our structure indicates that LIM kinases and actin should directly compete to interact with cofilin/ADF proteins. In the context of a cell, however, where actin is highly abundant and LIM kinases are less so, there is the possibility that direct competition might act as a feedback mechanism to fine tune control of actin dynamics by cofilin/ADF proteins.

Pre- and post-catalysis structures

An unusual feature of the co-crystal structure is the presence within the asymmetric unit of both pre- and post-catalysis complexes. While a detailed analysis of conformational changes associated with these states is not feasible because of the moderate resolution of the structure, we have highlighted some clear differences between the pre- and post-catalysis states (Figure 2). Although it is speculative that the precise differences represent initial conformational movements of a protein kinase following catalysis, the sum of the differences found in the DFG-motif, VAIK-motif, P-loop and nucleotide are suggestive of conformational changes in response to completion of catalysis, and correlate well with previous work (Bastidas et al., 2015). The unusual pre- and post-catalysis content of the asymmetric unit therefore seem to indicate initial steps undertaken in a protein kinase following following phosphate transfer that will ultimately lead to product release.

A previously unobserved mechanism of achieving high kinase-substrate fidelity

Systems-level mechanisms have been described for achieving kinase-substrate specificity, including expression levels, targeting, conditional docking sites, competition, localization and scaffolding proteins (Ubersax and Ferrell, 2007). At the molecular level, however, protein kinases achieve substrate specificity by broadly defined ‘docking’ and phosphosite ‘linear motif’ interactions (Bose et al., 2006; Goldsmith et al., 2007; Remenyi et al., 2006) (Figure 6A). Although many structures are available that show the interactions of protein kinases with linear motif peptides, fewer have been determined which describe the interaction of protein kinase domains with folded protein substrates. Comparison of $pLIMK1_{CAT}^{D460N}$:cofilin-1 with RIP3-MLKL (Xie et al., 2013), PKR-eIF2α (Dar et al., 2005) and CSK-Src (Levinson et al., 2008) kinase-protein substrate pairs demonstrates the distinct roles of canonical distal ‘docking’ and ‘linear motif’ recognition and helps define LIM kinase-cofilin as a distinct class of kinase-substrate complex (Figure S5). In each of the previous structures clear electron density reveals the molecular basis for their kinase-substrate distal docking interactions, which for these kinase domains is partially mediated by the αF-αG loop and helix αG, but no electron density is visible for their linear motif residues. In these and other kinase-substrate pairs, cooperation between docking and linear

motif sites is used to achieve high rates of phosphotransfer, with distal docking sites acting as molecular tethers that increase kinase-substrate affinity (Lieser et al., 2005; Ubersax and Ferrell, 2007). In contrast, LIM kinases phosphorylate a residue located at the N-terminus of cofilin/ADF proteins (Ser3) in the absence of extensive interactions with residues immediately flanking the phosphorylation site, with Ser3 being directly oriented to the correct position for catalysis by a complementary interaction between the LIM kinase C-lobe and cofilin helix α5 (Figure 6B). We therefore propose that the complementary cofilin α5 interaction with LIMK1 acts as the jig component of a 'molecular drill jig' that conformationally places cofilin residue Ser3 in exactly the correct location for phosphotransfer to occur (Figure 6C). The use of a highly specific molecular jig to target cofilin Ser3 for phosphorylation explains the exquisite selectivity observed for the LIM kinase sub-group towards cofilin/ADF proteins, and provides a mechanism by which protein kinases can achieve high fidelity towards their substrates.

EXPERIMENTAL PROCEDURES

Expression and purification pLIMK1$_{CAT}^{D460N}$ and cofilin-1

Human LIMK1 kinase domain (residues 329–638) containing point mutation D460N (LIMK1$_{CAT}^{D460N}$) was expressed in the baculovirus system. Following initial purification, LIMK1$_{CAT}^{D460N}$ was treated with recombinant PAK4 catalytic domain to phosphorylate it on Thr508 (pLIMK1$_{CAT}^{D460N}$) and further purified for co-crystallization. Wild type protein was used for kinase activity assays. Full-length human cofilin-1 (residues 2–166) was expressed in *E. coli* as a His$_6$-SUMO fusion protein and following tag removal by SUMO protease was further purified by ion exchange and size exclusion chromatography for co-crystallography.

Structure determination

For co-crystallization, pLIMK1$_{CAT}^{D460N}$ and cofilin-1 were mixed together and supplemented with AMP-PNP and $MgCl_2$. Crystals grew against precipitants in the range of 1.2–1.4 M sodium citrate, 0.1 M sodium acetate, pH 5.5, and were optimized by streak- or macro-seeding into fresh drops with lower precipitant concentration (1.0 – 1.2 sodium citrate). X-ray diffraction data were collected in 9 sweeps from 4 crystals at beamline 24-ID-E at the Advanced Photon Source. Data reduction was conducted using HKL2000 (Otwinowski and Minor, 1997), the structure determined by molecular replacement using Phaser (McCoy, 2007), refined using Refmac5 (Murshudov et al., 2011) and Phenix (Adams et al., 2010) and built using Coot (Emsley et al., 2010). Structure figures were prepared using CCP4mg (McNicholas et al., 2011).

In vitro kinase assay

Purified pLIMK1$_{CAT}$ or TESK1$_{CAT}$ was mixed with purified full-length cofilin in the presence of 0.1 μCi/ml ^{33}P-ATP. Reactions were carried out at 30° C for 10 minutes and quenched by addition of 1 mM EDTA-containing 1X SDS-loading buffer and resolved by SDS-PAGE. Autoradiography was used to detect the level of phosphorylated cofilin using a Bio-Rad Molecular Imager Fx system and Quantity One 1D Analysis software (Life Sciences Research). LIMK1 and cofilin mutants, and TESK1, were analyzed in this way.

Yeast growth assays

Serial dilutions of yeast harboring plasmids constitutively expressing N-terminal hexa-histidine tagged human cofilin-1 and inducibly expressing FLAG-tagged LIMK1 catalytic domain were plated on the appropriate selective media containing either glucose or galactose and incubated at either 25 ºC or 37 ºC as indicated.

Cofilin phosphorylation in mammalian cells

HEK293T cells were transfected with plasmids expressing N-terminally His_6-tagged cofilin (WT or mutant). Cells were harvested 36 hours post-transfection and analyzed by Western blotting using either rabbit anti-phosphocofilin (Ser3) (Cell Signaling, 1:3000 dilution) or mouse anti-His-tag (Sigma, 1:4000) primary antibodies. Samples were evaluated using a LiCor Odyssey Imaging system.

Supplementary Material

Refer to Web version on PubMed Central for supplementary material.

Acknowledgments

Staff at beamline 24-ID-E (NE-CAT-E) at the Advanced Photon Source, Argonne National Laboratory are thanked. We thank Anthony Koleske for sharing cDNA constructs, helpful discussions and critical analysis. We thank Dianqing Wu, Yiying Cai and Karin Reinisch for sharing cDNA constructs and vectors. We thank David Drubin for sharing yeast strains. Karen Anderson, John Asara, Ewa Folta-Stogniew and Rong Zhang are thanked. We thank Mark Lemmon, David Calderwood, Tom Pollard, Amy Stiegler, Clotilde Huet-Calderwood, Daniel Iwamoto, Xiaofeng Li and Byung Hak Ha for careful reading of the manuscript and insightful comments and suggestions. National Institutes of Health grants P41 GM103403 (NE-CAT beamline) and R01 GM102262 (B.E.T. and T.J.B.) funded the research.

References

Acevedo K, Li R, Soo P, Suryadinata R, Sarcevic B, Valova VA, Graham ME, Robinson PJ, Bernard O. The phosphorylation of p25/TPPP by LIM kinase 1 inhibits its ability to assemble microtubules. Exp Cell Res. 2007; 313:4091–4106. [PubMed: 18028908]

Adams JA. Kinetic and catalytic mechanisms of protein kinases. Chemical reviews. 2001; 101:2271–2290. [PubMed: 11749373]

Adams PD, Afonine PV, Bunkoczi G, Chen VB, Davis IW, Echols N, Headd JJ, Hung LW, Kapral GJ, Grosse-Kunstleve RW, et al. PHENIX: a comprehensive Python-based system for macromolecular structure solution. Acta Crystallogr D Biol Crystallogr. 2010; 66:213–221. [PubMed: 20124702]

Agnew BJ, Minamide LS, Bamburg JR. Reactivation of phosphorylated actin depolymerizing factor and identification of the regulatory site. J Biol Chem. 1995; 270:17582–17587. [PubMed: 7615564]

Amano T, Tanabe K, Eto T, Narumiya S, Mizuno K. LIM-kinase 2 induces formation of stress fibres, focal adhesions and membrane blebs, dependent on its activation by Rho-associated kinase-catalysed phosphorylation at threonine-505. Biochem J. 2001; 354:149–159. [PubMed: 11171090]

Andrianantoandro E, Pollard TD. Mechanism of actin filament turnover by severing and nucleation at different concentrations of ADF/cofilin. Mol Cell. 2006; 24:13–23. [PubMed: 17018289]

Arber S, Barbayannis FA, Hanser H, Schneider C, Stanyon CA, Bernard O, Caroni P. Regulation of actin dynamics through phosphorylation of cofilin by LIM-kinase. Nature. 1998; 393:805–809. [PubMed: 9655397]

Bamburg JR, McGough A, Ono S. Putting a new twist on actin: ADF/cofilins modulate actin dynamics. Trends Cell Biol. 1999; 9:364–370. [PubMed: 10461190]

Bastidas AC, Deal MS, Steichen JM, Guo Y, Wu J, Taylor SS. Phosphoryl transfer by protein kinase A is captured in a crystal lattice. J Am Chem Soc. 2013; 135:4788–4798. [PubMed: 23458248]

Bastidas AC, Wu J, Taylor SS. Molecular features of product release for the PKA catalytic cycle. Biochemistry. 2015; 54:2–10. [PubMed: 25077557]

Bernstein BW, Painter WB, Chen H, Minamide LS, Abe H, Bamburg JR. Intracellular pH modulation of ADF/cofilin proteins. Cell Motil Cytoskeleton. 2000; 47:319–336. [PubMed: 11093252]

Bhattacharyya RP, Remenyi A, Yeh BJ, Lim WA. Domains, motifs, and scaffolds: the role of modular interactions in the evolution and wiring of cell signaling circuits. Annu Rev Biochem. 2006; 75:655–680. [PubMed: 16756506]

Blanchoin L, Pollard TD. Interaction of actin monomers with Acanthamoeba actophorin (ADF/cofilin) and profilin. J Biol Chem. 1998; 273:25106–25111. [PubMed: 9737968]

Blanchoin L, Pollard TD. Mechanism of interaction of Acanthamoeba actophorin (ADF/Cofilin) with actin filaments. J Biol Chem. 1999; 274:15538–15546. [PubMed: 10336448]

Blanchoin L, Pollard TD, Mullins RD. Interactions of ADF/cofilin, Arp2/3 complex, capping protein and profilin in remodeling of branched actin filament networks. Curr Biol. 2000a; 10:1273–1282. [PubMed: 11069108]

Blanchoin L, Robinson RC, Choe S, Pollard TD. Phosphorylation of Acanthamoeba actophorin (ADF/cofilin) blocks interaction with actin without a change in atomic structure. J Mol Biol. 2000b; 295:203–211. [PubMed: 10623520]

Bose R, Holbert MA, Pickin KA, Cole PA. Protein tyrosine kinase-substrate interactions. Curr Opin Struct Biol. 2006; 16:668–675. [PubMed: 17085043]

Bravo-Cordero JJ, Magalhaes MA, Eddy RJ, Hodgson L, Condeelis J. Functions of cofilin in cell locomotion and invasion. Nat Rev Mol Cell Biol. 2013; 14:405–415. [PubMed: 23778968]

Dar AC, Dever TE, Sicheri F. Higher-order substrate recognition of eIF2alpha by the RNA-dependent protein kinase PKR. Cell. 2005; 122:887–900. [PubMed: 16179258]

De La Cruz EM. How cofilin severs an actin filament. Biophysical reviews. 2009; 1:51–59. [PubMed: 20700473]

Edwards DC, Sanders LC, Bokoch GM, Gill GN. Activation of LIM-kinase by Pak1 couples Rac/Cdc42 GTPase signalling to actin cytoskeletal dynamics. Nat Cell Biol. 1999; 1:253–259. [PubMed: 10559936]

Elam WA, Kang H, De la Cruz EM. Biophysics of actin filament severing by cofilin. FEBS Lett. 2013; 587:1215–1219. [PubMed: 23395798]

Emsley P, Lohkamp B, Scott WG, Cowtan K. Features and development of Coot. Acta Crystallogr D Biol Crystallogr. 2010; 66:486–501. [PubMed: 20383002]

Fedorov AA, Lappalainen P, Fedorov EV, Drubin DG, Almo SC. Structure determination of yeast cofilin. Nat Struct Biol. 1997; 4:366–369. [PubMed: 9145106]

Gibbs CS, Zoller MJ. Rational scanning mutagenesis of a protein kinase identifies functional regions involved in catalysis and substrate interactions. J Biol Chem. 1991; 266:8923–8931. [PubMed: 2026604]

Goldsmith EJ, Akella R, Min X, Zhou T, Humphreys JM. Substrate and docking interactions in serine/threonine protein kinases. Chemical reviews. 2007; 107:5065–5081. [PubMed: 17949044]

Ha BH, Davis MJ, Chen C, Lou HJ, Gao J, Zhang R, Krauthammer M, Halaban R, Schlessinger J, Turk BE, et al. Type II p21-activated kinases (PAKs) are regulated by an autoinhibitory pseudosubstrate. Proc Natl Acad Sci U S A. 2012; 109:16107–16112. [PubMed: 22988085]

Iida K, Moriyama K, Matsumoto S, Kawasaki H, Nishida E, Yahara I. Isolation of a yeast essential gene, COF1, that encodes a homologue of mammalian cofilin, a low-M(r) actin-binding and depolymerizing protein. Gene. 1993; 124:115–120. [PubMed: 8440472]

Kanamori T, Suzuki M, Titani K. Complete amino acid sequences and phosphorylation sites, determined by Edman degradation and mass spectrometry, of rat parotid destrin- and cofilin-like proteins. Archives of oral biology. 1998; 43:955–967. [PubMed: 9877327]

Klejnot M, Gabrielsen M, Cameron J, Mleczak A, Talapatra SK, Kozielski F, Pannifer A, Olson MF. Analysis of the human cofilin 1 structure reveals conformational changes required for actin binding. Acta Crystallogr D Biol Crystallogr. 2013; 69:1780–1788. [PubMed: 23999301]

Kraus MH, Issing W, Miki T, Popescu NC, Aaronson SA. Isolation and characterization of ERBB3, a third member of the ERBB/epidermal growth factor receptor family: evidence for overexpression

in a subset of human mammary tumors. Proc Natl Acad Sci U S A. 1989; 86:9193–9197. [PubMed: 2687875]

Lappalainen P, Fedorov EV, Fedorov AA, Almo SC, Drubin DG. Essential functions and actin-binding surfaces of yeast cofilin revealed by systematic mutagenesis. EMBO J. 1997; 16:5520–5530. [PubMed: 9312011]

Laskowski RA. PDBsum new things. Nucleic Acids Res. 2009; 37:D355–359. [PubMed: 18996896]

Levinson NM, Seeliger MA, Cole PA, Kuriyan J. Structural basis for the recognition of c-Src by its inactivator Csk. Cell. 2008; 134:124–134. [PubMed: 18614016]

Li R, Soosairajah J, Harari D, Citri A, Price J, Ng HL, Morton CJ, Parker MW, Yarden Y, Bernard O. Hsp90 increases LIM kinase activity by promoting its homo-dimerization. FASEB J. 2006; 20:1218–1220. [PubMed: 16641196]

Lieser SA, Aubol BE, Wong L, Jennings PA, Adams JA. Coupling phosphoryl transfer and substrate interactions in protein kinases. Biochim Biophys Acta. 2005; 1754:191–199. [PubMed: 16213199]

Maekawa M, Ishizaki T, Boku S, Watanabe N, Fujita A, Iwamatsu A, Obinata T, Ohashi K, Mizuno K, Narumiya S. Signaling from Rho to the actin cytoskeleton through protein kinases ROCK and LIM-kinase. Science. 1999; 285:895–898. [PubMed: 10436159]

McCoy AJ. Solving structures of protein complexes by molecular replacement with Phaser. Acta Crystallogr D Biol Crystallogr. 2007; 63:32–41. [PubMed: 17164524]

McNicholas S, Potterton E, Wilson KS, Noble ME. Presenting your structures: the CCP4mg molecular-graphics software. Acta Crystallogr D Biol Crystallogr. 2011; 67:386–394. [PubMed: 21460457]

Mezna M, Wong AC, Ainger M, Scott RW, Hammonds T, Olson MF. Development of a high-throughput screening method for LIM kinase 1 using a luciferase-based assay of ATP consumption. J Biomol Screen. 2012; 17:460–468. [PubMed: 22156225]

Mizuno K. Signaling mechanisms and functional roles of cofilin phosphorylation and dephosphorylation. Cell Signal. 2013; 25:457–469. [PubMed: 23153585]

Mizuno K, Okano I, Ohashi K, Nunoue K, Kuma K, Miyata T, Nakamura T. Identification of a human cDNA encoding a novel protein kinase with two repeats of the LIM/double zinc finger motif. Oncogene. 1994; 9:1605–1612. [PubMed: 8183554]

Moon AL, Janmey PA, Louie KA, Drubin DG. Cofilin is an essential component of the yeast cortical cytoskeleton. J Cell Biol. 1993; 120:421–435. [PubMed: 8421056]

Morgan TE, Lockerbie RO, Minamide LS, Browning MD, Bamburg JR. Isolation and characterization of a regulated form of actin depolymerizing factor. J Cell Biol. 1993; 122:623–633. [PubMed: 7687605]

Moriyama K, Iida K, Yahara I. Phosphorylation of Ser-3 of cofilin regulates its essential function on actin. Genes to cells : devoted to molecular & cellular mechanisms. 1996; 1:73–86. [PubMed: 9078368]

Murshudov GN, Skubak P, Lebedev AA, Pannu NS, Steiner RA, Nicholls RA, Winn MD, Long F, Vagin AA. REFMAC5 for the refinement of macromolecular crystal structures. Acta Crystallogr D Biol Crystallogr. 2011; 67:355–367. [PubMed: 21460454]

Niwa R, Nagata-Ohashi K, Takeichi M, Mizuno K, Uemura T. Control of actin reorganization by Slingshot, a family of phosphatases that dephosphorylate ADF/cofilin. Cell. 2002; 108:233–246. [PubMed: 11832213]

Ojala PJ, Paavilainen VO, Vartiainen MK, Tuma R, Weeds AG, Lappalainen P. The two ADF-H domains of twinfilin play functionally distinct roles in interactions with actin monomers. Mol Biol Cell. 2002; 13:3811–3821. [PubMed: 12429826]

Okano I, Hiraoka J, Otera H, Nunoue K, Ohashi K, Iwashita S, Hirai M, Mizuno K. Identification and characterization of a novel family of serine/threonine kinases containing two N-terminal LIM motifs. J Biol Chem. 1995; 270:31321–31330. [PubMed: 8537403]

Oser M, Yamaguchi H, Mader CC, Bravo-Cordero JJ, Arias M, Chen X, Desmarais V, van Rheenen J, Koleske AJ, Condeelis J. Cortactin regulates cofilin and N-WASp activities to control the stages of invadopodium assembly and maturation. J Cell Biol. 2009; 186:571–587. [PubMed: 19704022]

Otwinowski, Z.; Minor, W. Processing of X-ray diffraction data collected in oscillation mode. In: Carter, CW.; Sweet, RM., editors. Methods in Enzymology. San Diego: Academic Press New York; 1997. p. 307-326.

Paavilainen VO, Oksanen E, Goldman A, Lappalainen P. Structure of the actin-depolymerizing factor homology domain in complex with actin. J Cell Biol. 2008; 182:51–59. [PubMed: 18625842]

Poukkula M, Kremneva E, Serlachius M, Lappalainen P. Actin-depolymerizing factor homology domain: a conserved fold performing diverse roles in cytoskeletal dynamics. Cytoskeleton (Hoboken). 2011; 68:471–490. [PubMed: 21850706]

Remenyi A, Good MC, Lim WA. Docking interactions in protein kinase and phosphatase networks. Curr Opin Struct Biol. 2006; 16:676–685. [PubMed: 17079133]

Ressad F, Didry D, Xia GX, Hong Y, Chua NH, Pantaloni D, Carlier MF. Kinetic analysis of the interaction of actin-depolymerizing factor (ADF)/cofilin with G- and F-actins. Comparison of plant and human ADFs and effect of phosphorylation. J Biol Chem. 1998; 273:20894–20902. [PubMed: 9694836]

Rosok O, Pedeutour F, Ree AH, Aasheim HC. Identification and characterization of TESK2, a novel member of the LIMK/TESK family of protein kinases, predominantly expressed in testis. Genomics. 1999; 61:44–54. [PubMed: 10512679]

Scott RW, Olson MF. LIM kinases: function, regulation and association with human disease. Journal of molecular medicine. 2007; 85:555–568. [PubMed: 17294230]

Shi F, Telesco SE, Liu Y, Radhakrishnan R, Lemmon MA. ErbB3/HER3 intracellular domain is competent to bind ATP and catalyze autophosphorylation. Proc Natl Acad Sci U S A. 2010; 107:7692–7697. [PubMed: 20351256]

Skamnaki VT, Owen DJ, Noble ME, Lowe ED, Lowe G, Oikonomakos NG, Johnson LN. Catalytic mechanism of phosphorylase kinase probed by mutational studies. Biochemistry. 1999; 38:14718–14730. [PubMed: 10545198]

Toshima J, Ohashi K, Okano I, Nunoue K, Kishioka M, Kuma K, Miyata T, Hirai M, Baba T, Mizuno K. Identification and characterization of a novel protein kinase, TESK1, specifically expressed in testicular germ cells. J Biol Chem. 1995; 270:31331–31337. [PubMed: 8537404]

Ubersax JA, Ferrell JE Jr. Mechanisms of specificity in protein phosphorylation. Nat Rev Mol Cell Biol. 2007; 8:530–541. [PubMed: 17585314]

Van Troys M, Huyck L, Leyman S, Dhaese S, Vandekerkhove J, Ampe C. Ins and outs of ADF/cofilin activity and regulation. Eur J Cell Biol. 2008; 87:649–667. [PubMed: 18499298]

Williams DM, Cole PA. Proton demand inversion in a mutant protein tyrosine kinase reaction. J Am Chem Soc. 2002; 124:5956–5957. [PubMed: 12022825]

Xie T, Peng W, Yan C, Wu J, Gong X, Shi Y. Structural insights into RIP3-mediated necroptotic signaling. Cell reports. 2013; 5:70–78. [PubMed: 24095729]

Yang EJ, Yoon JH, Min DS, Chung KC. LIM kinase 1 activates cAMP-responsive element-binding protein during the neuronal differentiation of immortalized hippocampal progenitor cells. J Biol Chem. 2004; 279:8903–8910. [PubMed: 14684741]

Yang N, Higuchi O, Ohashi K, Nagata K, Wada A, Kangawa K, Nishida E, Mizuno K. Cofilin phosphorylation by LIM-kinase 1 and its role in Rac-mediated actin reorganization. Nature. 1998; 393:809–812. [PubMed: 9655398]

Yonezawa N, Nishida E, Iida K, Yahara I, Sakai H. Inhibition of the interactions of cofilin, destrin, and deoxyribonuclease I with actin by phosphoinositides. J Biol Chem. 1990; 265:8382–8386. [PubMed: 2160454]

Yount RG, Babcock D, Ballantyne W, Ojala D. Adenylyl imidodiphosphate, an adenosine triphosphate analog containing a P--N--P linkage. Biochemistry. 1971; 10:2484–2489. [PubMed: 4326768]

Zhao H, Hakala M, Lappalainen P. ADF/cofilin binds phosphoinositides in a multivalent manner to act as a PIP(2)-density sensor. Biophys J. 2010; 98:2327–2336. [PubMed: 20483342]

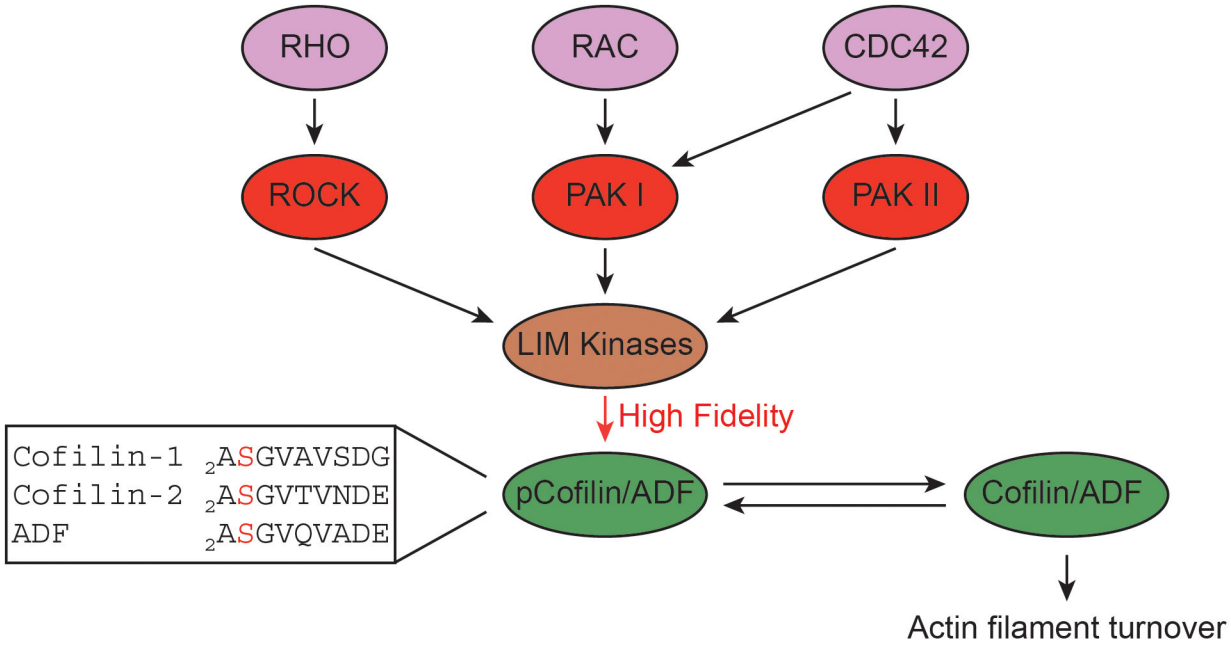

Figure 1. Schematic showing the role of a high fidelity kinase-substrate pair in control of actin polymerization

Control of actin filament dynamics is regulated by the upstream RHO-GTPase family and their effector proteins, which directly activate the LIM kinases. The LIM kinases phosphorylate the cofilin/ADF-family of proteins on residue Ser3. Sequence alignment for residues 2–10 is shown for human cofilin-1, cofilin-2 and ADF proteins; Ser3 is marked in red. Unphosphorylated cofilin/ADF proteins bind and destabilize actin filaments, however, cofilin/ADF proteins phosphorylated on Ser3 do not bind actin. Cofilin phosphorylation is a major convergence point that links upstream signaling to actin remodeling. See also Figure S1.

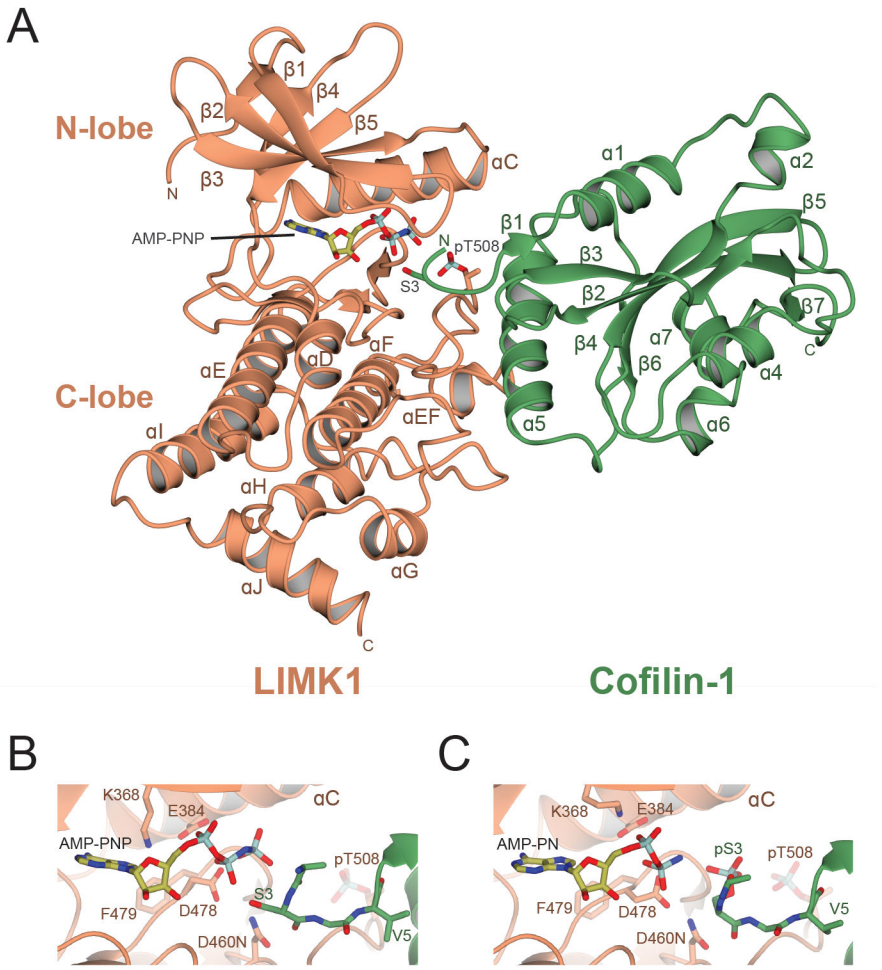

Figure 2. Co-crystal structure of the LIMK1 catalytic domain in complex with full-length cofilin-1

(A) Overall structure of pLIMK1$_{CAT}^{D460N}$ with cofilin-1. LIMK1 is shown in brown, and cofilin-1 in green. Secondary structure elements, N- and C- termini, kinase N- and C-lobes are labeled. Cofilin Ser3, phosphorylated LIMK1 activation loop residue pT508, and bound nucleotide are shown in stick format. **B, C)** Close up of the active site for pre-catalytic (B) and post-catalytic (C) complexes found in the asymmetric unit. LIMK1 residues shown in stick format are from the conserved kinase DFG-motif (D478, F479), HRD-motif (D460N), catalytic lysine (K368) and catalytic glutamate (E384). N-terminal residues of cofilin-1 are shown in stick format. See also Figure S2.

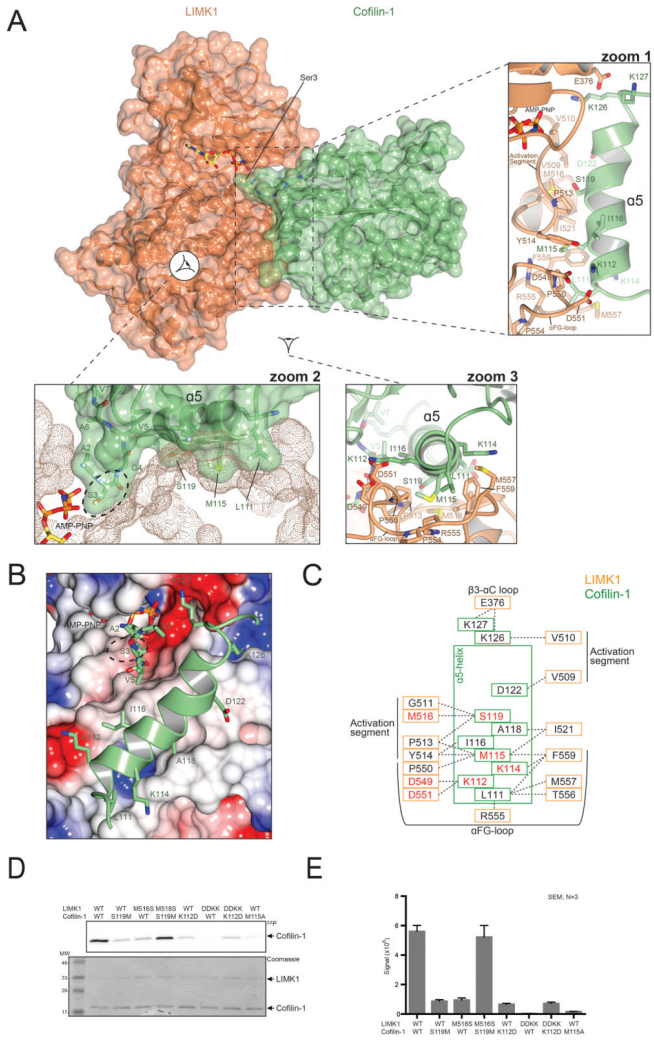

Figure 3. Molecular basis for LIMK1 recognition of its substrate cofilin-1

(A) Detailed interaction between pLIMK1$_{CAT}^{D460N}$ with cofilin-1. Surface renderings of LIMK1 (brown) and cofilin-1 (green). Top right and bottom right zoomed regions show details of the interaction, with side chains shown in stick format. Residues and some secondary structure elements are labeled. Bottom left shows the surface of LIMK1 illustrating the deep cleft that cofilin helix α5 residues insert into. Ser3 is indicated by a dashed oval. **B)** Electrostatic potential of interaction interface. Face on view of LIMK1 (electrostatic potential) and cofilin (only helix α5 and the N-terminal residues shown). Side chains and nucleotide shown in stick format, and helix α5 in cartoon format. Ser3 is indicated by a dashed oval. **C)** Map of LIMK1:Cofilin interactions. Residues involved in kinase-substrate targeting are shown; LIMK1 in brown and cofilin in green. Residues mutated in this study are indicated with red text. Interactions indicated with dotted lines. Structure elements indicated. Interactions defined by PDBSum (Laskowski, 2009). **D)** *In vitro* phosphorylation of cofilin-1 by LIMK1. Autoradiography showing pLIMK1$_{CAT}$ phosphorylation of full-length Cofilin-1 (top). Mutants are indicated. Loading indicated by Coomassie stained SDS-PAGE (bottom). **E)** Quantitation of kinase assay. N=3. S.E.M.

indicated. Comparison to wild-type shows that all pairs except $LIMK1_{CAT}^{M516S}$/cofilin^{S119M} are statistically significant (p-value < 0.0005) (paired t-test type 2). See also Figure S3.

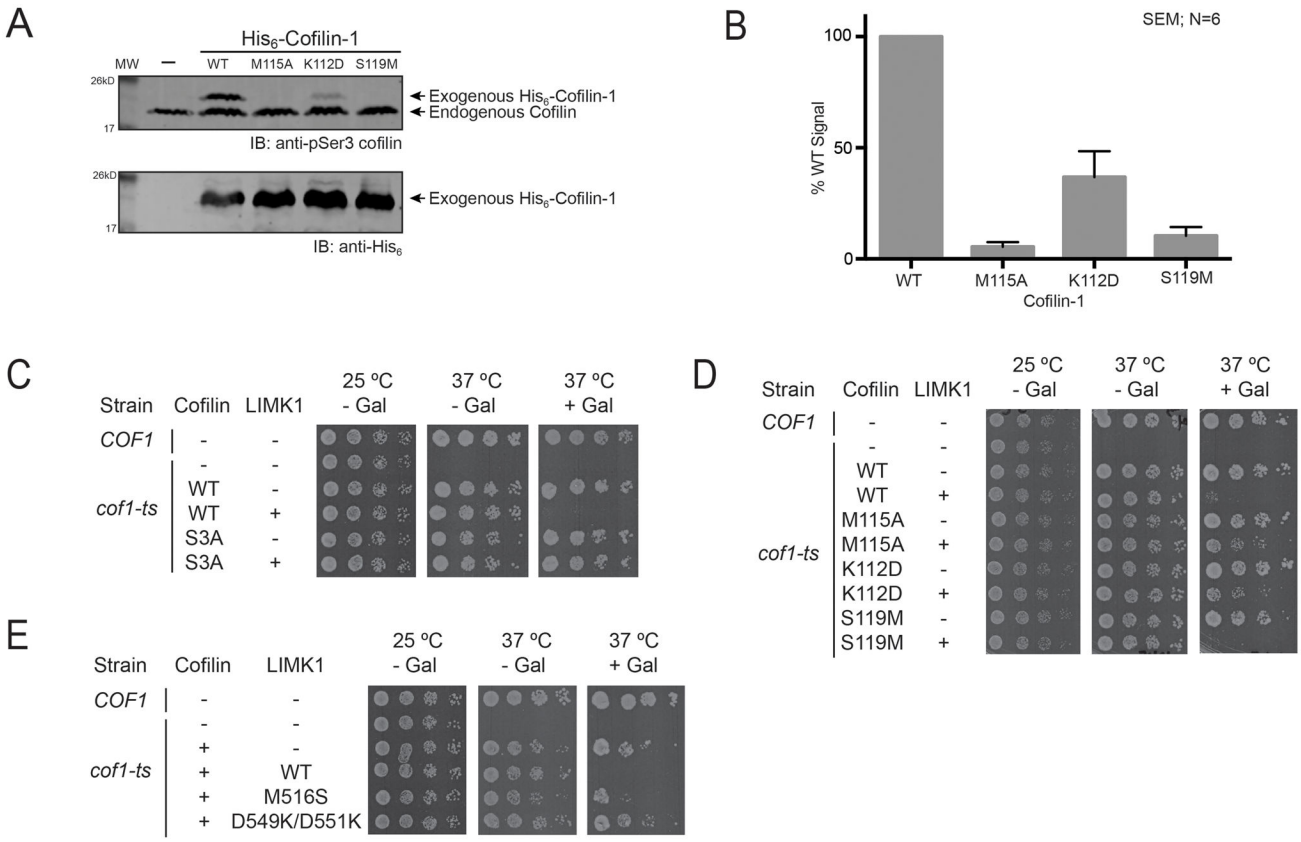

Figure 4. Disruption of LIMK1-cofilin-1 interaction in mammalian cells and yeast

(A) Cofilin phosphorylation in mammalian cells. N-terminally His-tagged cofilin ran slower by SDS-PAGE than endogenous cofilin, allowing internal validation by anti-cofilin pSer3 antibody that the endogenous LIM kinases are active. HEK293T cells. **B)** Quantitation of exogenous pSer3 cofilin-1. Percent of wild-type signal calculated per experiment, and averaged across experiments. N=6. S.E.M. indicated. All pairings to wild-type are statistically significant (p-value < 0.0003) (paired t-test type 2). **C)** Expression of $LIMK1_{CAT}$ in yeast is toxic to cells dependent on human cofilin-1. Serial dilutions of the indicated yeast strains harboring plasmids expressing human cofilin-1 (WT or S3A mutant) and human $LIMK1_{CAT}$ or the corresponding empty vectors were plated on solid media in the presence of glucose (-Gal) or galactose (+Gal) to induce $LIMK1_{CAT}$ expression. Plates were grown at the indicated temperature for 2 days (glucose plates) or 4 days (galactose plate). **D–E)** Growth of *cof1-ts* cells co-expressing cofilin-1 or $LIMK1_{CAT}$ mutants. Cells harboring the indicated cofilin-1 (D) or $LIMK1_{CAT}$ (E) mutant plasmids were grown as in (C).

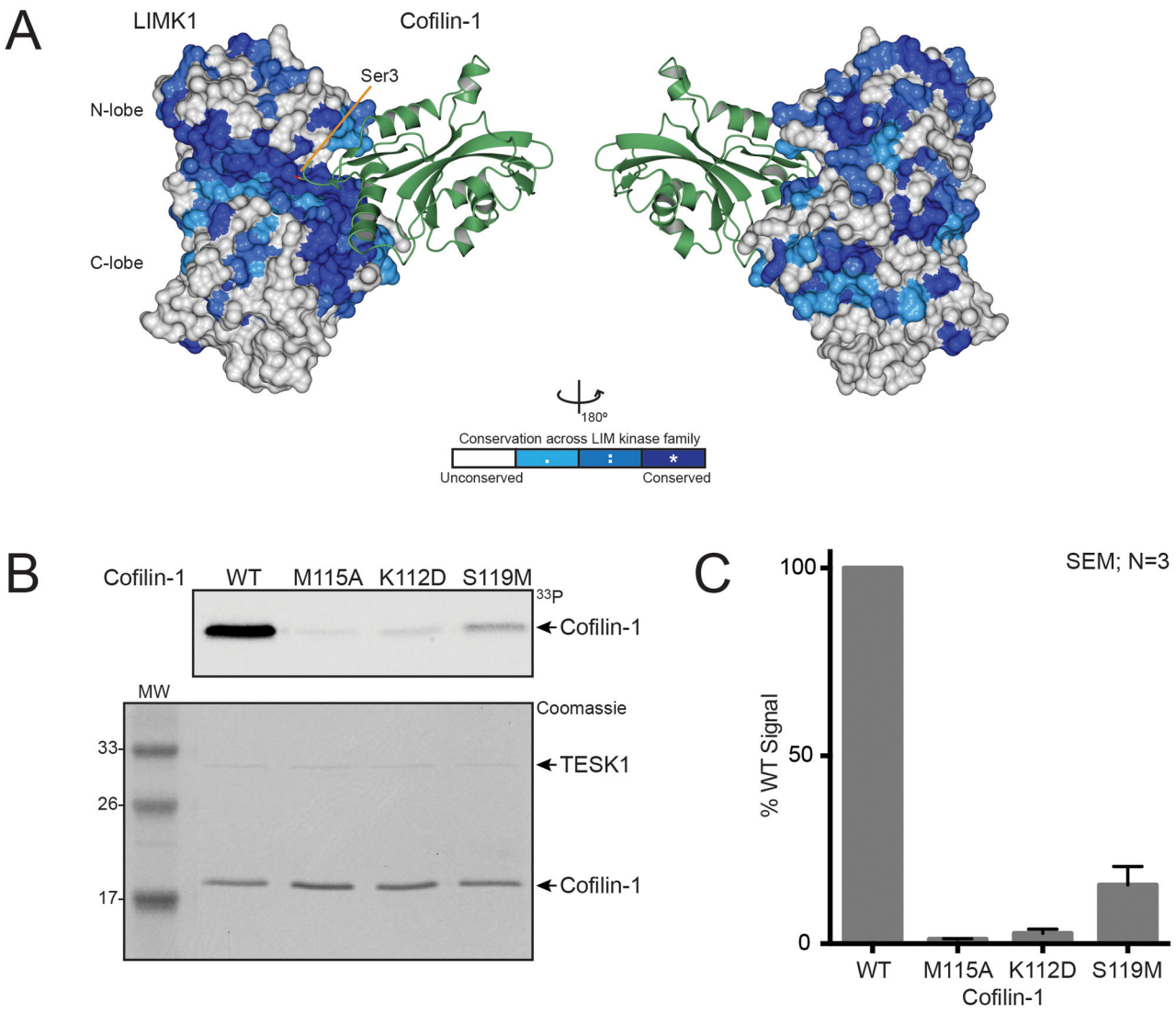

Figure 5. Conservation of the high fidelity kinase-substrate pair across the LIM kinase family

(A) Conservation of LIMK1. Surface representation of LIMK1 structure indicating conservation across the human LIM kinases (LIMK1, LIMK2, TESK1, and TESK2). Dark blue indicates complete conservation (see Figure S5). Cofilin shown in cartoon format in green. **B)** *In vitro* kinase assay. $TESK1_{CAT}$ phosphorylation of cofilin-1 or cofilin-1 mutants analyzed by autoradiography (top). Loading analyzed by Coomassie stained SDS-PAGE (bottom). **C)** Quantitation of kinase assay. N=3. S.E.M. indicated. Comparison to wild-type pair shows that all pairings are statistically significant (p-value < 0.0001) (paired t-test type 2). See also Figure S4.

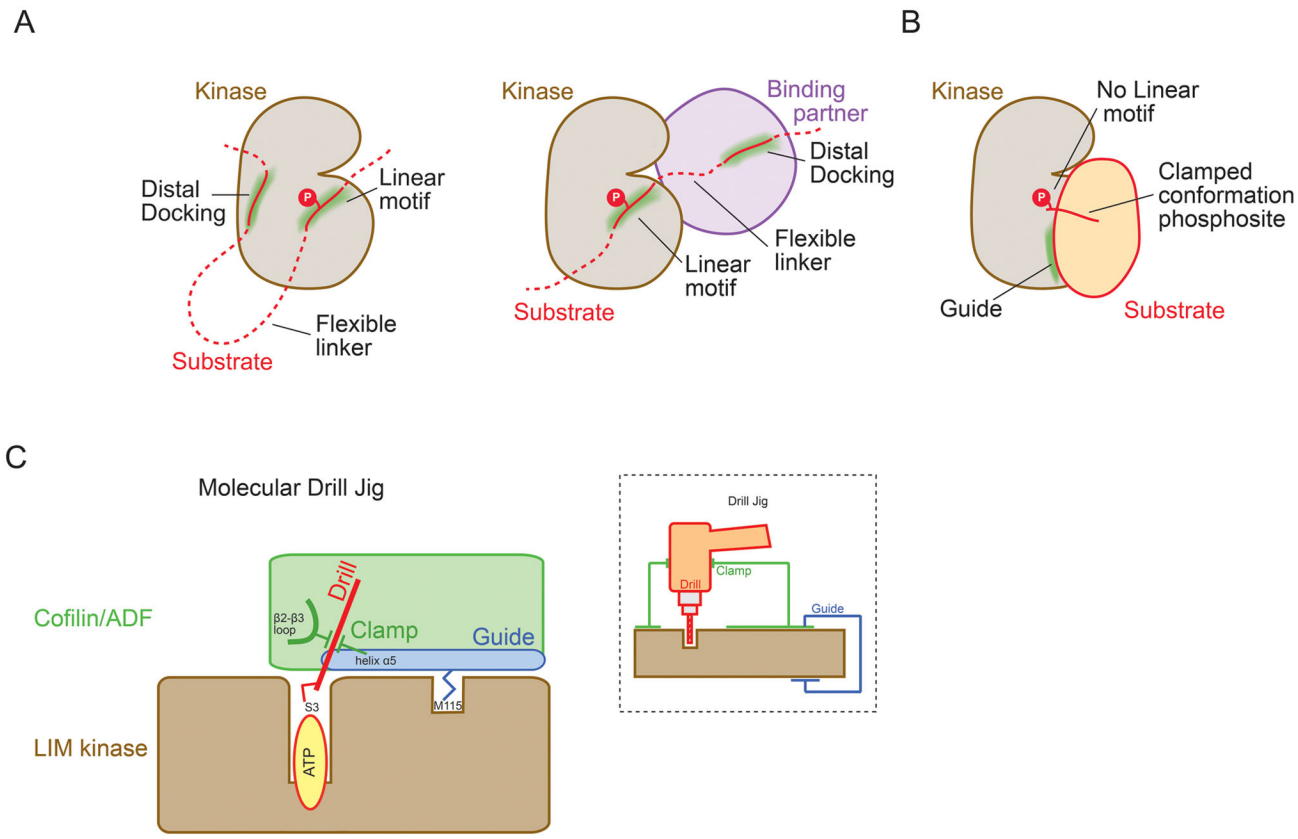

Figure 6. The cofilin 'molecular drill jig' as a mechanism to achieve high kinase-substrate fidelity

(A) Schematic diagram showing the canonical molecular level mechanisms by which kinase-substrate specificity is achieved. Distal docking and linear motif sites are indicated. **B)** Schematic for how LIM kinases achieve high fidelity phosphorylation of cofilin/ADF proteins, an alternative mechanism to achieve molecular level specificity for kinase-substrate pairs. **C)** The complementary kinase-substrate interaction between LIM kinases and cofilin/ADF proteins acts as the jig component of a 'molecular drill jig', which conformationally places cofilin residue Ser3 in the correct location for catalysis. See also Figure S5.

Table 1

Data collection and refinement statistics.

	pLIMK1$_{CAT}^{D460N}$:Cofilin-1	**LIMK1$_{CAT}^{D460N}$**
PDB accession code	**5HVK**	**5HVJ**
Data Collection		
Space group	$P2_12_12_1$	$P2_1$
X-ray source	APS, 24-ID-E (NE-CAT-E)	APS, 24-ID-E (NE-CAT-E)
Number crystals	4	2
Cell dimensions, *a*, *b*, *c* (Å)	81.1, 102.3, 141.9	55.0, 59.6, 98.3
α, *β*, *γ* (°)	90, 90, 90	90, 101.3, 90
Wavelength (Å)	0.97918	0.97918
Resolution range (Å) *	50.0 – 3.5 (3.63 – 3.50)	50.0 – 2.2 (2.28 – 2.20)
No. unique reflections	15,631	31,929
Degrees of data (°)	394	720
Completeness (%) *	100.0 (100.0)	100.0 (100.0)
R_{pim} (%) *	26.1 (76.3)	4.9 (27.1)
$I/\sigma I$ *	2.5 (1.3)	12.8 (1.1)
Redundancy *	10.1 (8.5)	14.3 (13.3)
Wilson *B*-factor (Å^2)	33.7	42.2
Refinement		
Resolution range (Å) *	48.1 – 3.5 (3.72 – 3.50)	40.0 – 2.2 (2.26 – 2.20)
R_{factor} (%) *	27.3 (33.6)	20.6 (37.7)
Free R_{factor} (%) *	31.0 (36.7)	25.2 (44.0)
No. Free *R* reflections *	783 (120)	1613 (145)
Chain identifiers of complexes built	pLIMK1:pCofilin:AMP-PN (A:B:F) pLIMK1:Cofilin:AMP-PNP (C:D:E)	LIMK1:AMP-PNP (A:C) LIMK1 (B)
Residue range built	pLIMK1 A: 324–487; 501–634 pCofilin B: 2–166 pLIMK1 C: 328–486; 501–633 Cofilin D: 2–165	A: 329–485, 508–633 B: 330–484, 509–637
No. water molecules	0	70
Model Quality		
RMSD bond lengths (Å)	0.003	0.002
RMSD bond angles (°)	0.763	0.641
Overall *B* (all atoms) (Å^2)	39.3	75.1
B (Å^2)		
(protein)	A: 33.3, B: 47.8, C: 31.3, D: 56.7	A: 68.7 B: 82.0
(water)	--	55.8
(nucleotide)	E: 49.8, F: 41.3	C: 114.0

	pLIMK1$_{CAT}^{D460N}$:Cofilin-1	**LIMK1$_{CAT}^{D460N}$**
PDB accession code	**5HVK**	**5HVJ**
Ramachandran plot (%) favored/allowed/outliers	94.9/5.1/0.0	97.0/3.0/0.0
MolProbity score/percentile	2.2/100%	1.76/95%

* Parentheses indicate highest resolution shell

AMP-PN indicates AMP-PNP lacking the gamma phosphate